Chapter 12

Fluid-driven Cyclic Propagation of a Joint in the Ithaca Siltstone, Appalachian Basin, New York

Alfred Lacazette[1] *and Terry Engelder*

Department of Geosciences, The Pennsylvania State University, University Park, PA 16802, U.S.A.

[1] *Present address: Texaco Inc., Exploration and Production Technology Dept., 3901 Briarpark, Houston, TX 77042, U.S.A.*

Abstract

Crack-seal veins, millifractures, and joints with rhythmic c-type plume patterns are common examples of cyclic crack propagation in rocks. Although in some cases cyclic propagation could result from periodic external forcing by far-field stress changes or fluid-pressure pulsation, the regularity and rhythmic nature of several types of fractures suggest that cyclic propagation also arises from dynamic instability of the fracture–fluid–rock system. A 40–90-m-long cross-fold joint that propagated within a single bed of the Devonian Ithaca Siltstone near Watkins Glen, New York has a plumose surface morphology with multiple arrest lines indicating that cracking occurred in increments rather than in one smooth rupture. The crack increments increase in overall length in the propagation direction over the final 28-m portion of the exposed end of the study joint with the largest increments increasing in length from 0.6 m to 1.0 m. At least three conceptual models based on linear elastic fracture mechanics and fluid flow along joints can be imagined to explain incremental crack growth under conditions of constant stress and pore pressure: the compressibility-limited propagation model; the flow-limited propagation model; and the infiltration-limited propagation model. This surface morphology of the study joint provides constraints on the propagation process so that the growth of the joint may be analyzed in terms of these three models. Based on quantitative evaluation of the cracking process, compressibility-limited propagation is favored and the driving fluid is identified as a gas rather than a brine. The gas is identified as a natural gas on the basis of geological constraints.

FAULT MECHANICS AND TRANSPORT PROPERTIES OF ROCKS
ISBN 0-12-243780-2

1. Introduction

The morphology of joints and veins in rocks suggests that crack propagation sometimes occurs in spurts during either reactivation of open ruptures or repeated cracking through a narrow zone which subsequently fills with vein material. For example, crack-seal veins consist of the repeated overgrowth of cements in new crack traces which followed old (Ramsay, 1980). These overgrowths are seeded in crystallographic continuity on the surface of cracks which themselves may have propagated through previous overgrowth. The crossing pattern of millifractures in Mesozoic limestones of the Italian Apennines (Geiser and Sansone, 1981) and in carbonates of the Central Appalachians also indicate repeated rupture. Millifractures are seen as hairline cracks often associated with the development of disjunctive cleavage in limestones throughout foreland fold–thrust belts. Crack-seal veins and millifractures may differ only by the fact that millifractures do not propagate through or follow existing veins. A prominent feature on the surface of joints within Devonian shales and siltstones of the Appalachian Plateau is a regular pattern of fan-shaped plumose markings (rhythmic c-type plumes)* indicating propagation and arrest through many cycles either horizontally within a single bed (Bahat and Engelder, 1984), or vertically between beds (Helgeson and Aydin, 1988, 1989). Hence, cyclic propagation is a feature that crack-seal veins, millifractures, and joints with rhythmic c-type plumes all have in common. The stress which drives these cracks appears to develop by an increase of the crack fluid pressure which momentarily exceeds the total stress acting inward from the surrounding rock by an amount that is sufficient to overcome the resistance of the rock to fracture propagation. This form of fluid-induced crack growth is a type of natural hydraulic fracturing (Secor, 1965; Beach, 1977; Engelder, 1985, Engelder and Lacazette, 1990).

The extremely uniform orientation of many joint and vein sets and the regularity of episodic fracturing implied by crack-seal veins and joints with rhythmic c-type plumes is striking. From these observations we conclude that it is unlikely that such regular, cyclic propagation was caused by repeated reactivation under varying conditions of tectonic stress or catastrophic injection of pulses of high-pressure fluid from an external source. Our notion is that cyclic crack propagation represents a momentary disequilibrium in the local crack–fluid–rock system followed quickly by a return to stable conditions. If so, crack interactions or other mechanisms can cause a crack to become unstable under conditions of constant remote stress and matrix pore pressure.

This chapter presents detailed observations of incremental growth of a vertical joint contained in a single bed of Devonian siltstone in the Appalachian plateau near Ithaca New York, U.S.A. To explain these observations we consider three conceptual models for this type of natural hydraulic fracturing and conclude that the compressibility of the fluid within the joint was responsible for cyclic crack propagation and that the joint was driven by a gas, which geologic evidence suggests was natural gas.

2. Incremental Crack Growth in the Ithaca Siltstone

Joints in the Ithaca siltstone at Watkins Glen, New York formed by in-situ natural hydraulic fracturing (Engelder and Lacazette, 1990). The origin flaws were 1–3 cm fossils

* c-Type plumes belong to a class of joint surface morphology with curved or irregular plume axes (Bahat and Engelder, 1984).

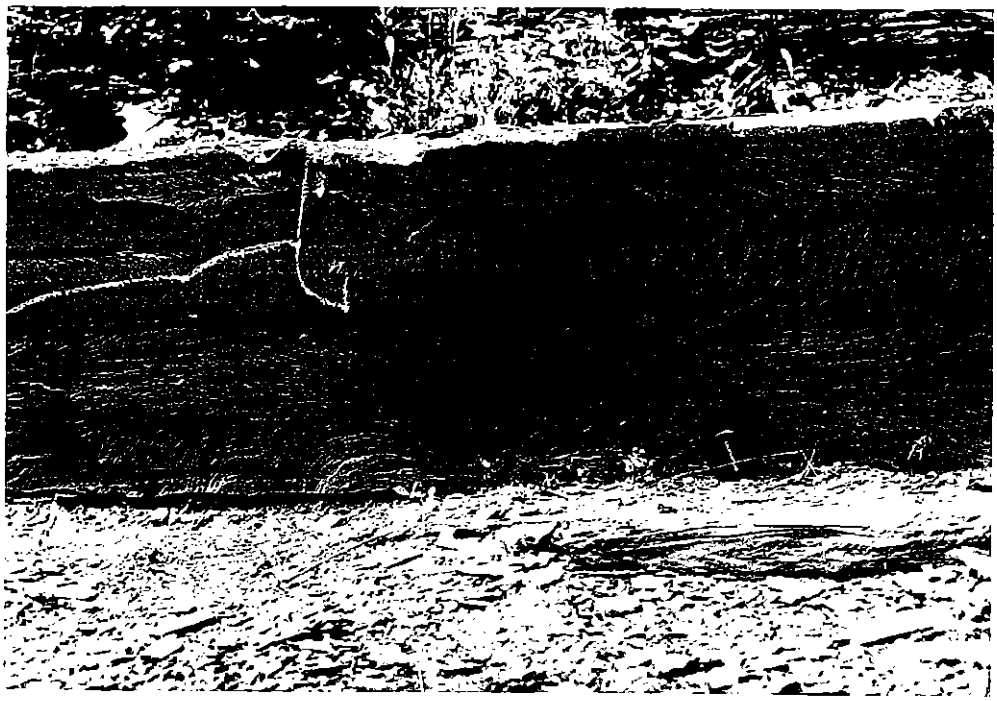

Figure 1. Photograph of joint initiation point in the Ithaca Siltstone at Watkins Glen, New York.

and flute casts (Bahat and Engelder, 1984; Engelder and Lacazette, 1990). Calculations using linear elastic fracture mechanics and poroelasticity theory (assuming 3 km of overburden) show that the vertical stress and pore pressure were about 80 and 65 MPa, respectively, at the time of joint formation (Engelder and Lacazette, 1990).

Rhythmic c-type plume patterns indicate that joints propagated in discrete increments (Bahat and Engelder, 1984). These patterns are well-developed on the surfaces of cross-fold joints in exposures of essentially flat-lying Devonian siltstones of the Ithaca Formation at Watkins Glen, New York (Bahat and Engelder, 1984; Engelder, 1986; Engelder, 1987). Joints in siltstones of the Ithaca Formation are vertical and are restricted to individual beds that are always less than 1 m thick. Siltstone beds are separated from each other by laminas of shale or thick shale beds. Composite joints cutting both siltstones and shales have vertical dimensions up to at least 10 m (Helgeson and Aydin, 1989). The initiation point of the fractures are found by tracing fan-like patterns of delicate barbs or hackles back to a central origin (Figure 1, photograph of initiation point). The hackles sometimes end abruptly at the perimeter of the fan, indicating that the crack arrested. Successive propagation increments are characterized by a smooth area beyond the previous arrest line which gives way to progressively more intense hackle so that another fan is developed beyond the point of arrest of the previous event (Figure 2, photograph of propagation cycle). The point of arrest of the crack front is again marked by the abrupt cessation of hackle. Although some joints in the siltstones show rhythmic c-type plumes, others show s-type plumes (Bahat and Engelder, 1984) which are characterized by a continuous plume without detectable arrest lines. Individual joints are highly planar and maintain a very consistent orientation.

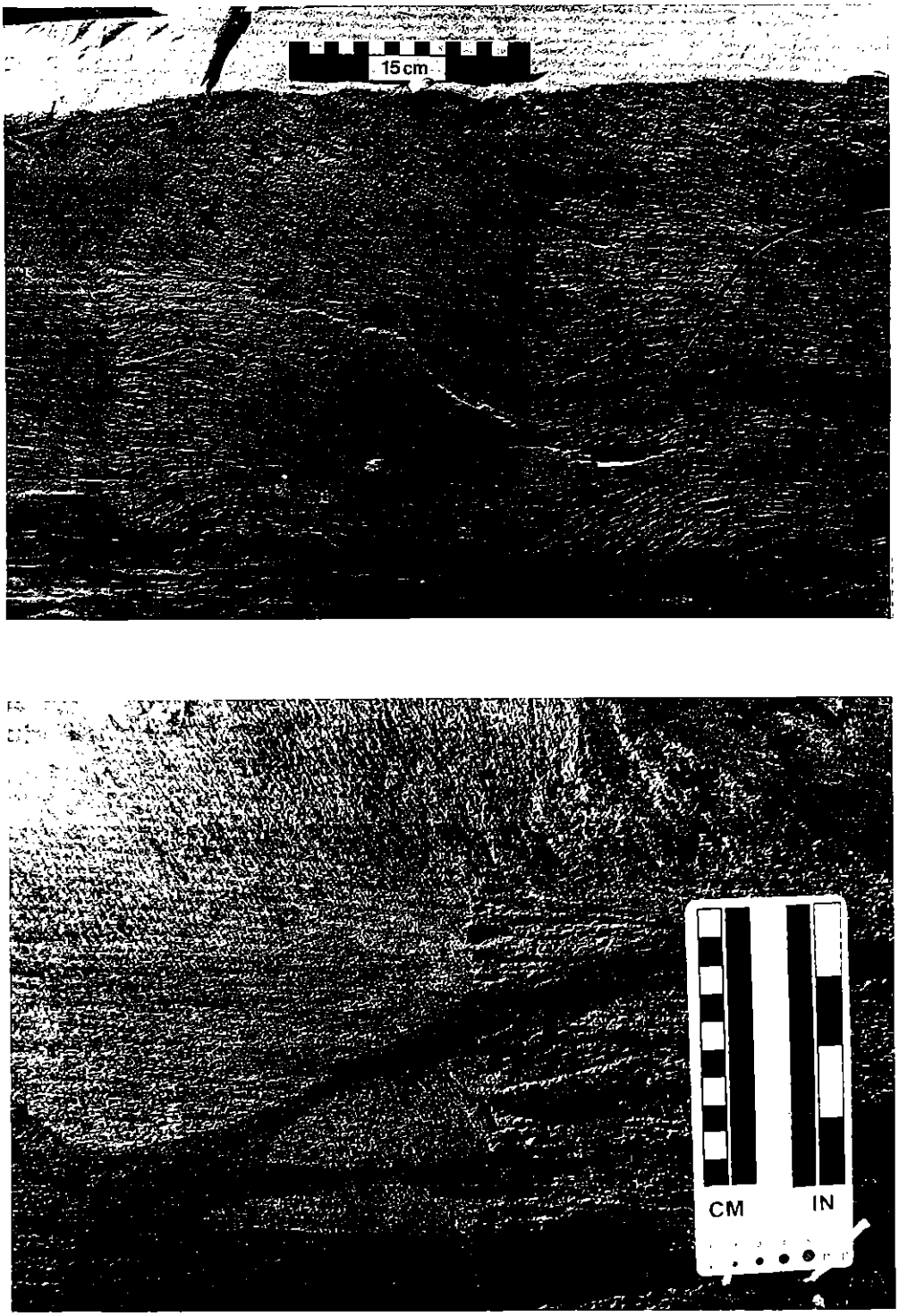

Figure 2. *Top*, photograph of propagation cycles in the Ithaca siltstone. *Bottom*, close up of arrest line showing the sharp boundary between coarse and fine hackle.

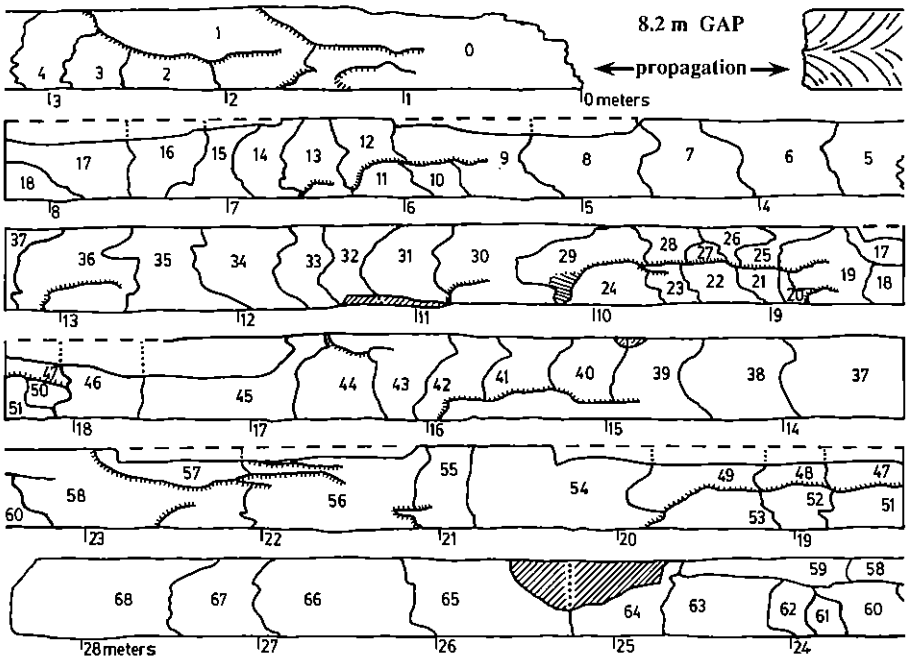

Figure 3. Map drawn from photographs of the surface of a vertical joint contained in a siltstone bed that is isolated in shale at Watkins Glen, New York. The fracture propagated in discrete increments which are numbered in order of development as determined by morphological criteria. Arrest lines as shown mark the position of the fracture front at the termination of each fracturing cycle. The study joint initiated within the 8.2-m gap and propagated outwards. A 3.6-m segment of the study joint surface to the northwest (right) of the gap contains an S-type plume (Bahat and Engelder, 1984). Tick marks show where side-cracks rejoin the main fracture plane. Diagonal lines indicate local destruction of surface morphology by weathering. Dashed lines and dotted lines respectively show the inferred location of the top of the bed and the arrest line where parts of the bed are missing or weathered. Successive map segments match up exactly where they terminate in vertical lines whereas open segment ends indicate slight overlap between segments. See text for further discussion.

To further understand the mechanism of incremental crack growth, the surface of one well-exposed cross-fold joint (hereafter referred to as 'the study joint') in the Ithaca Formation was mapped in detail from photographs. A map of the joint surface is given in Figure 3. The increments are numbered in order of their propagation sequence as determined by observations of the surface morphology. A map of the exposed part of the upper surface of the bed that contains the study joint is given in Figure 4. The study joint was confined to a 0.41-m-thick bed and contained 68 separate propagation increments. It terminated in solid rock. During road construction, one wall of the study joint was ripped away so that the terminal arrest line is both preserved and exposed (Figure 3). The arrest lines of each increment and other surface features of the study joint were marked with chalk. This surface was then photographed with scales so that the area of each fracture increment could be determined from the photographs with a digital planimeter in the laboratory. Replicate determinations of increment areas on

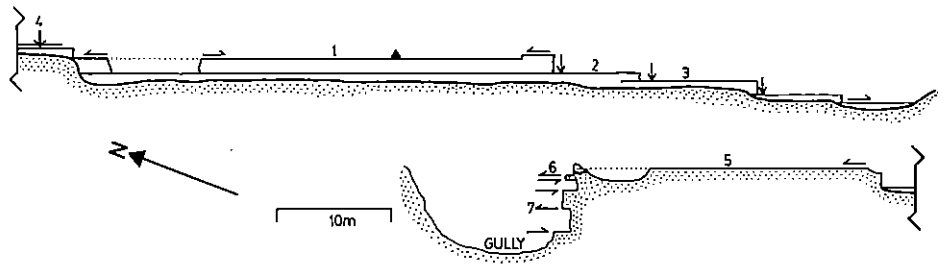

Figure 4. Map of the exposed parts of the upper surface of the siltstone bed containing the study joint shown in Figure 3. Arrows show the location of initiation points, joints propagated outwards from the initiation points. Half-arrows show the propagation direction of joints where the initiation point is not contained in the exposed surface. Joint 1 is that shown in Figure 3. Only joint 1 shows arrest lines. All other joints in the bed show S-type plumes (Bahat and Engelder, 1984). Solid triangle shows the location of segment 45 where the study joint undergoes a slight change of orientation. Joint 2 is the location of the measurements of joint surface morphology of Brown and Scholz (1985). Note that joint 3 terminates just north of its initiation point indicating asymmetrical propagation. Joints 1, 3, and 5 show terminal arrest lines. '4' denotes the intersection point of two approximately coplanar joints with opposite propagation directions.

different photographs with different scales shows that the areas thus determined are repeatable to $\pm 0.015\ m^2$. We find that the mean bed thickness from direct measurements in the field is 0.443 ± 0.046 m. The average bed thickness determined using the cumulative areal measurements and the measured joint length is 0.41 m, which is within the range of the independently measured bed thickness. The area of each fracture increment was converted to a normalized increment length by dividing increment areas by the average bed thickness (0.41 m). Figure 5 gives the increment area plotted against the increment number as given in Figure 3. Figure 3 was prepared from smaller-scale photographs than those used for the area determinations given in Figure 5. The delicate surface morphology of the joints at this outcrop is rapidly being degraded by weathering. Portions of the surface layer either had peeled off or were in the process of peeling when this study was undertaken and the studied joint face may soon be rendered unusable for mapping.

The overall orientation of the study joint is 338/86, although it changes slightly at increment 45 (Figure 3). This increment has a relatively rough and broken-up surface unlike the smooth surface of the rest of the study joint. Southeast of increment 45 the study joint strikes counterclockwise to and dips more shallowly by 1° or less than the remainder of the face, which lies to the northwest of this increment.

Although the surface of the study joint is quite planar and smooth overall, *side-cracks* propagate away from the main joint surface (Figures 3 and 6). Side-cracks are always clockwise to the main fracture face and deviate from its orientation by up to roughly 1°. Where side-cracks leave the main fracture, the hackle is continuous and the surface is smooth, planar, and unbroken. A distinct change of orientation cannot be detected at the point of departure from the main fracture. In general, side-cracks terminated within solid rock after propagating for a short distance and the septum of rock that separated the main fracture from the side-crack (if one ever existed) has broken away so that the entire surface of the side-crack is exposed and the connecting fracture is at

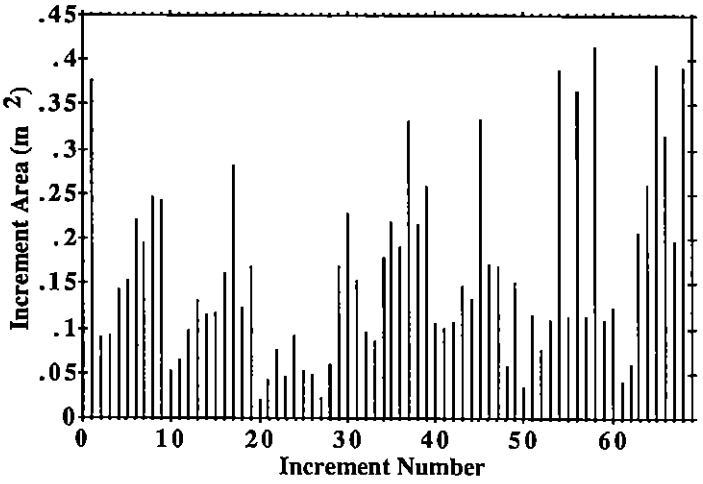

Figure 5. Surface area of increments shown in Figure 4 as determined by digital planimetry of photographs in the laboratory. Repeat determinations on different photographs show that the areas are reproducible to $\pm 0.015\ m^2$.

a high counterclockwise angle to the main fracture face. In one or two cases large side-cracks propagated far enough so that up to 1 cm of rock separates the side-crack tip from the main fracture and the entire surface of the side crack is not exposed (these cracks can be traced on the top surface of the bed). At a few locations the side-cracks smoothly rejoin the main fracture surface so that no distinct break is present, although the surfaces of reconnection are more steeply inclined to the main fracture face than the remainder of the side-crack. These areas are indicated by long tic marks with or without associated arrest lines (see increments 29 and 0, Figure 3). Side-cracks always resulted in a tongue which ran ahead of the main face along either the top or the bottom of the bed prior to arrest. Although the arrest lines of fracturing events that did not result in side-cracks have an overall tendency towards being convex in the propagation direction (see increments 4, 5, 8, 30–34, 66–68), they also show a tendency to propagate farther along the surfaces of the bed (see increments 6, 7, 17).

On the basis of the surface morphology of the study joint and other field observations we draw six major conclusions regarding incremental propagation:

(1) *Crack velocity increased during each propagation event.* The fan pattern accompanying incremental growth is characterized by a subtle increase in intensity of the barbs or hackles up to the point of their abrupt termination. Based on the fractography of ceramics, this increase in intensity of the barbs or hackles suggests an increase in crack velocity (Kulander et al., 1979; Kulander and Dean, 1985). Although it is argued below that the joints in the Ithaca Siltstone propagated in a quasi-static manner, the crack velocity must have increased until halting abruptly.

(2) *Incremental crack growth is quasistable.* If a crack becomes unstable it can accelerate up to about 0.38 times the shear-wave velocity of the material (Broek, 1987). Crack branching may occur after the fracture has reached or exceeded 0.13–0.19 times the shear wave velocity (Broek, 1987). During incremental growth of joints in the Ithaca Formation there is no evidence for this type of high-velocity crack branching. We reject

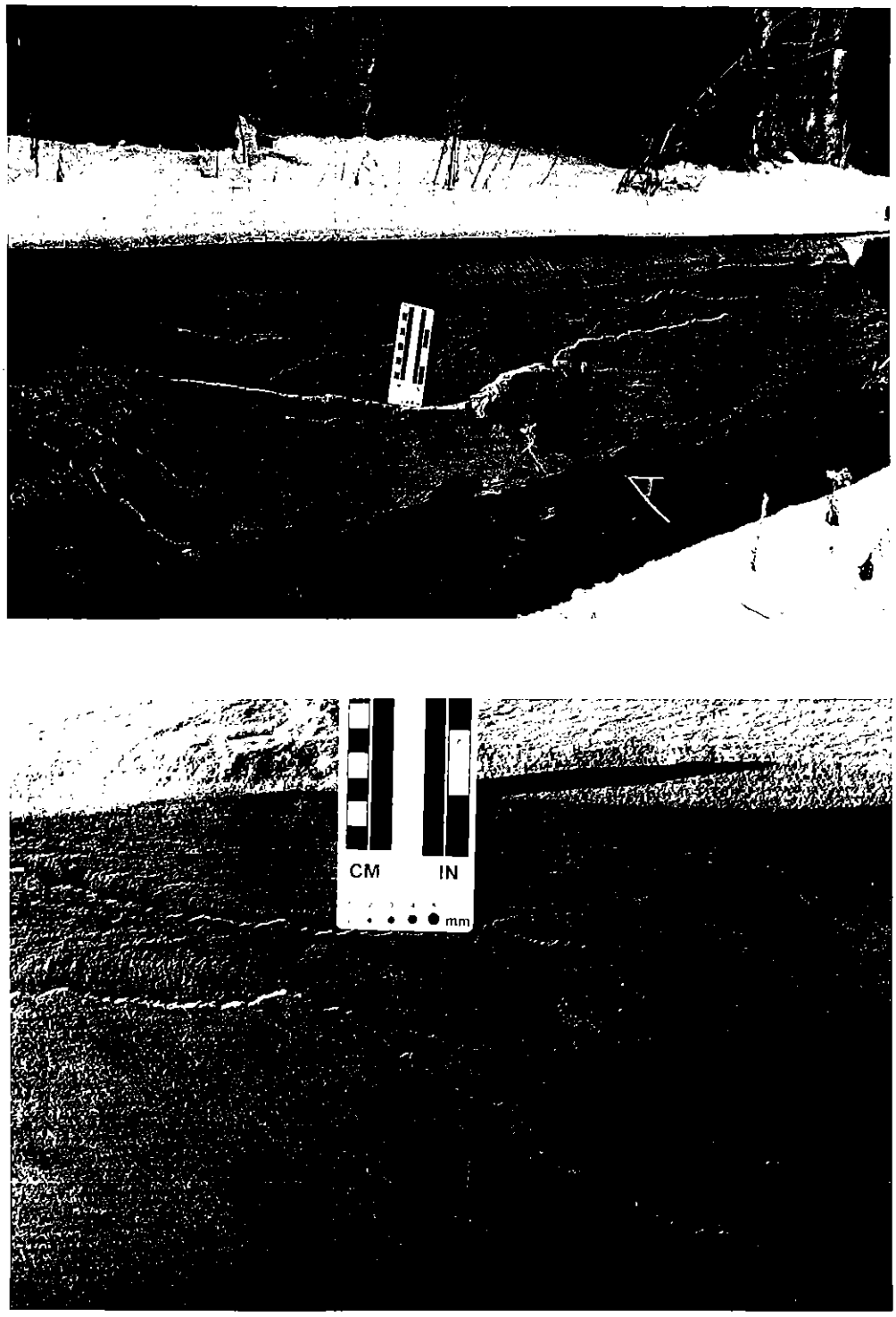

Figure 6. Photographs of the side-crack of increments 56 and 57. *Top*, entire side-crack. *Bottom*, departure point of the side-crack in increment 56.

the hypothesis that the side-cracks represent branching associated with high-velocity fracture propagation for several reasons. (i) The side-cracks themselves are quite planar and show no tendency to curve or fork (Figure 6). (ii) Side-cracks are sometimes contained entirely within an increment so that they must have developed prior to the peak velocity of the fracture as indicated by the maximum intensity of hackle development adjacent to the arrest line (see increments 0, 36, 58; Figure 3) yet side-cracks do not develop near the arrest lines of these same increments. (iii) No increase of hackle development is observed at the point of deviation of side-cracks, rather the hackle intensity continues to smoothly increase in intensity toward the arrest lines of both the side-crack and the main fracture (Figure 6). Therefore a local velocity increase cannot have lead to branching. (iv) Branches typically subtend an angle of about 15° relative to the main fracture (Broek, 1987), which is more than an order of magnitude greater than the observed angle subtended by side cracks.

Although evidence indicates that the study joint was a relatively low-velocity fracture, propagation of each increment ends abruptly without the large number of very fine cracks in complex en echelon patterns as is found at the termination of stable cracks in granite (e.g., Segall and Pollard, 1983). This may also indicate a sudden termination after acceleration. The lack of branches only implies that velocities sufficient to generate branches were not achieved. The crack could have become unstable and propagated under conditions of K_I close or equal to K_{IC}.

(3) *The initial propagation increment was large.* Although 13 or 14 other joints are contained within the adjacent exposed portion of the same bed (Figure 4) only the study joint shows a rhythmic c-type plume. Within the outcrop as a whole, joint faces showing rhythmic c-type plumes are much less common than joints showing s-type plumes. The morphology of the study joint shown in Figure 3 suggests that the apparent scarcity of rhythmic c-type plumes may result from large initial propagation increments relative to the parts of the joints showing cyclic increments in the majority of cases. Hence, one is more likely to observe the initial increment on the relatively small preserved and/or exposed portions of the joints. The propagation direction of the study joint was clearly outwards from the missing segment (increment 0) and the portion to the northwest of the missing segment does not show arrest lines. Also, increment 0 is much larger than any of the succeeding increments. These observations suggest that the initial propagation event occurred as a single continuous rupture between 13.5 and 20 m in total length (assuming symmetrical propagation about the initiation point) and that the arrest line that divides increment 0 from increment 1 was the first arrest line to form on the exposed portion of the study joint. Because most of the exposed portions of other joints within this bed contain initiation points and are much shorter than the study joint, only the large initial increments may be presently observable.

(4) *The study joint propagated under conditions of significant differential stress.* The combination of extreme planarity and close spacing of the joints at this outcrop indicate that these fractures propagated under conditions of significant differential stress so that the crack parallel far-field compressive stresses were large relative to the crack normal stress (Olson and Pollard, 1989). The tendency of these fractures to develop planar side-cracks may be indicative of propagation at or near the limit of pure tensile failure (see Jaeger and Cook, 1979 for a discussion of hybrid tensile–shear failure). Alternatively, temporary perturbations of the stress field resulting from minor interactions with an adjacent joint, material inhomogeneities, or other causes could have produced minor deviations of the crack path. The constancy of orientation of the entire joint, the total

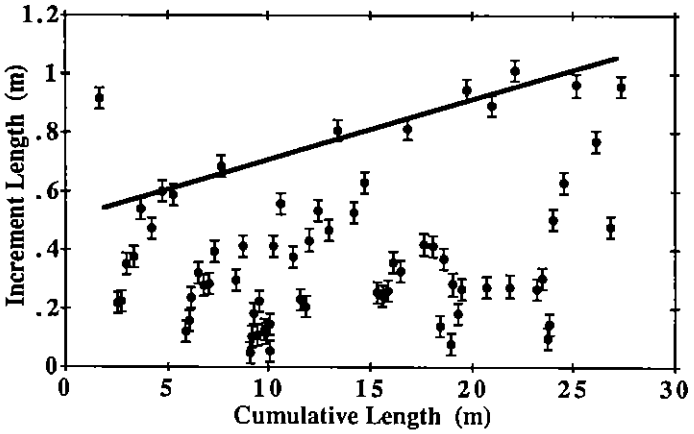

Figure 7. Normalized length of each fracture increment, with error bars, vs. cumulative length of the study joint surface shown in Figure 4. Normalized lengths were computed by measuring the area of each fracture increment on photographs and dividing by the bed thickness (0.41 m). Note the tendency for the largest increments to increase in size with increasing joint length.

absence of side-cracks from many increments, the small number and size of side-cracks relative to the entire joint, and the tendency of some side-cracks to smoothly rejoin the main fracture face all indicate that the great majority of the study joint formed as a pure mode I fracture.

(5) *The maximum size of the increments increased as the study joint grew.* Figure 7 shows the normalized length of fracture increments vs. the cumulative length. Normalized lengths were calculated from the area data of Figure 5 by dividing by the bed thickness (0.41 m). (Note that no attempt was made to include the extra fracture surface area represented by side-cracks in the computation of the normalized increment lengths when compiling the data for Figures 5 and 7.) Figure 5 shows that the length of successive fracture increments increases and decreases in a cyclical pattern. However, comparison with Figure 3 shows that small increments occur after side-crack-forming events. For example, increments 2–4 and increments 40–42 formed after side-cracking events and are especially small. Post-side-crack increments may be smaller because after side-crack formation the crack front is configured as a corner crack rather than as an edge crack and the geometric factor (see eq. (4)) is larger (Tada et al., 1973; Murakami, 1987), which favors failure at a lower driving stress. Increments which do not immediately follow side-cracking events have surface areas between 0.10 and 0.43 m^2, whereas the surface areas of increments that follow side-cracking events are generally less than 0.10 m^2 and always less than 0.15 m^2 in size. Increments that followed side-cracking events must therefore be considered anomalous because they represent a variable and much smaller degree of instability than events that began at fairly even through-the-bed arrest lines. One prominent feature of these data is the presence of a uniformly sloping cut-off at large increment lengths above which no data are present (Figure 7). This cut-off is composed of the largest increments which began at uniform, straight arrest lines. These show the most regular behavior and, hence, are most indicative of changing fracture behavior. Increment 1, which is an apparent exception to this rule, is discussed in a later section.

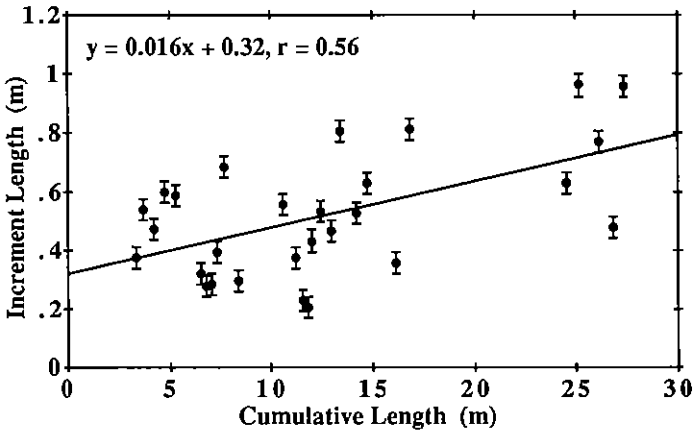

Figure 8. Linear best fit to normalized length vs. cumulative normalized length data for increments that did not follow side-cracking events.

Figure 8 shows the same data as Figure 7 but with the data points of post-side-crack increments removed and a linear best fit to the data. Although the data show substantial scatter, the correlation coefficient of 0.56 indicates that a significant amount of the variation in increment length is correlated with increasing joint length. The overall increment size is thus seen to increase with increasing joint length as well as the maximum increment size.

(6) *The total length of the study joint is less than 90 m.* Figure 4 shows a map of the bed containing the study joint and its location within the bed. Although the study joint is concealed to the north of the missing section, all but two of the joints that are exposed in the gully at the north end of the bed have propagation directions opposite to that of the north section of the study joint and one of them (joint 6) is not continuous to the south. The remaining one (joint 7) is approximately coplanar with joint 1 but cannot be confidently correlated with any points in the southern portion of the bed because of the length of the covered section and because of the tendency of these joints to undergo slight changes in orientation along their lengths. It is therefore possible that joint 7 is the northern section of joint 1.

The bed that contains the joints thins slightly from the location of joint 1 towards the north and appears to pinch out or undergo a lateral change in lithology in the gully. In either case, neither the bed nor the joints are present on the north side of the gully, so that joint 1 had a maximum possible length of about 90 m.

3. Conceptual Models for Incremental Crack Growth

This section describes a set of three conceptual models to define the ways in which natural hydraulic fractures may be driven. Quantitative application of the models leads to predictions of increment size and to the stress cycling that occurs during propagation. The models do not treat the problem of initiation of an incremental propagation event. Sammis and Julian (1987) show that an isolated flat crack in compression that is loaded by internal fluid pressure cannot propagate unstably. If cyclic propagation is to occur

by any of the mechanisms described below, then some mechanism must allow excess fluid pressure to build up within the joint. Any such mechanism must release the joint so that an unstable increment may develop with $K_I \geq K_{IC}$, and so that the fracture accelerates as it propagates.

Although interactions between cracks within a set may be important for releasing a restrained crack tip, our models assume no crack interaction during the propagation event. Other types of cycling mechanism include far-field stress variation and/or pulses of fluid injected into either the fracture or the pore space of the rock mass from an external reservoir. The following models are end-member idealizations and real fractures may combine elements of all of them. All of these models allow for propagation at either a single crack tip or simultaneously at both crack tips.

To drive the crack, fluid pressure inside the joint must counterbalance both the total earth stress acting perpendicular to the crack and fracture toughness effects (eq. 8). On the rapid timescale of joint propagation we assume that changes in driving stress are solely a function of internal crack pressure. Therefore, the four major parameters controlling driving stress are: (1) increases in joint volume during joint propagation; (2) flow from pore space in the host rock to the joint; (3) compressibility of the fluid within the joint; (4) flow within the joint including flow from the main body of the joint into the newly created portion of the joint tip. The first parameter acts to decrease driving stress whereas the next two act to maintain driving stress. The fourth controls both the timescale of the stress drop and the stress distribution within the joint. By applying these four parameters in various combinations, one can imagine three qualitative models for incremental joint propagation: the infiltration-limited model; the compressibility-limited model; and the flow-limited model (Figure 9).

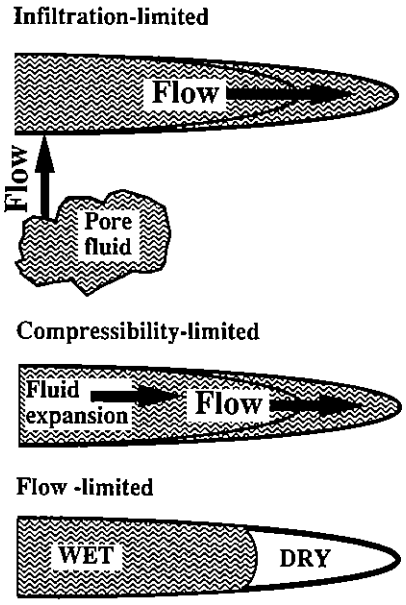

Figure 9. Schematic illustration of the three conceptual models for the hydraulic control of crack propagation. The velocity vs. stress intensity regions appropriate to each model are shown in Figure 12. See text for discussion.

Infiltration-limited propagation

Infiltration-limited propagation is described elsewhere (i.e., Segall and Pollard, 1983). The infiltration-limited model assumes that the driving fluid is incompressible. The rate of infiltration of fluid into the joint from adjacent pore space in the host rock maintains fluid pressure to counterbalance total stress and fracture toughness. Throughout propagation K_I remains at a level where crack growth can occur and joint propagation is stable.

Using fracture mechanics, Secor (1965, 1969) and Engelder and Lacazette (1990) predict that the internal pressure required to extend a joint decreases as the joint grows. The pressure decline occurs because of decreasing influence of fracture toughness with increased joint size (eqs. 4 and 5). Furthermore, infiltration resulting from growth of a joint set may lead to decreased remote pore pressure and thus to a decline in the poroelastic component of the crack perpendicular stress (eq. 5). If the rock volume around the joint is not instantaneously recharged, the increase of the joint volume due to growth must decrease the fluid pressure within a joint. Hence one consequence of joint growth is the development of a fluid pressure gradient between the joint and the pore space of the rock mass. Pore fluid spontaneously drains into the joint. The internal pressure may thereby be maintained at a level sufficient to cause joint propagation. Joint growth is arrested either when the rock mass pore pressure drops below the level required to cause crack propagation or when the far-field earth stress changes. A pore pressure decrease could be caused either by drainage of pore fluid into the joints of the growing joint set or by drainage of the rock mass through the joint system into another region of the rock mass.

Steady-state, stable crack growth occurs if the rate of fluid flow into the joint is sufficient to maintain internal pressure so that the joint slowly grows, where $K_I \leq K_{IC}$ and the fluid pressure is equal throughout the joint. In this case, the rate of fluid flow into the joint is equal to the rate of increase of the joint volume due to growth.

Incremental crack growth may occur if circumstances allow the crack to become unstable where $K_I > K_{IC}$. The size of the increment produced by unstable propagation is limited by the pore volume of the rock surrounding the crack that is hydraulically connected to the fracture on the timescale of fracture propagation. The size of the hydraulically connected region will be controlled by a combination of porosity and permeability of the wall rock, and crack velocity. Arrest occurs once the increase of fracture volume decreases the fluid pressure so that $K_I < K_{IC}$. Recharge of the adjacent host rock and joint follows arrest. During this period of infiltration the fluid pressure within the joint increases.

The infiltration-limited model predicts that during incremental growth the crack velocity will gradually decline as the pressure within the joint declines. The porosity and permeability of the Ithaca Siltstone are so small (Table 1) that only very small increments could form by this mechanism. This model is therefore discarded as a mechanism of cyclic cracking and incremental growth in this case. However, infiltration-limited propagation is considered to cause continuous slow crack propagation during the development of the first increment of the study joint.

Compressibility-limited propagation

Expansion of the fluid within the joint can maintain the crack driving stress even though propagation causes an increase in crack volume. For our compressibility-limited model, propagation distance during a rupture event is a function of the compressibility of the

Table 1. Physical properties of the Ithaca Siltstone

Property	Value	Orientation[a]
Bulk density	2620 kg m^{-3}	
Young's modulus	56 GPa	BN
Young's modulus	73 GPa	BP
Intrinsic compressibility	1.3×10^{-11} Pa^{-1}	BP
Bulk compressibility	4.8×10^{-11} Pa^{-1}	BP
Biot's constant (α)	0.7	BP
Poisson's Ratio (ν)[b]	0.17	BN
Permeability	<0.01 md	BP
Porosity	<2%	
$K_{IC}(c_C = 82\ mm)$[c]	2.66 MPa $m^{1/2}$	BN
$K_{IC}(c_C = 11\ mm)$	1.74 MPa $m^{1/2}$	BN
$K_{IC}(c_C = 2\ mm)$	1.26 MPa $m^{1/2}$	BN
$K_{IC}(c_C = 80\ mm)$	2.02 MPa $m^{1/2}$	BP
$K_{IC}(c_C = 11\ mm)$	1.31 MPa $m^{1/2}$	BP

Data from A. Lacazette; I. Meglis; Scott (1989); and Evans et al. (1989).
[a] BP, bedding parallel; BN, bedding normal.
[b] Measurement of ν taken from a silty mudstone of the West River Formation.
[c] c_C, Critical crack length at the onset of rapid crack propagation.

fluid within the joint. In this model, rates of fluid flow into the newly created portion of the joint are equal to or greater than the speed of joint propagation. Thus fluid pressure changes at an equal rate within all portions of the joint at all times during the fracturing process. This model also assumes that infiltration into the joint from pores in the host rock is insignificant during propagation. Arrest occurs because the increase in joint volume due to crack growth will eventually reduce the fluid pressure within the entire joint until the fluid drive is counterbalanced by fracture toughness and the crack perpendicular compressive stress.

If this model applies, then the ratio of new joint volume to old joint volume remains constant, so that each successive increment is slightly larger than the preceding one. Such a ratio applies because the size of each increment is controlled by the compressibility of the fluid within the joint. For example, a joint that is filled with gas should show larger increments than one that is filled with water. If the fluid is a gas-saturated brine, then the increment size will depend on the solubility of the gas in the brine and on the relative compressibilities of the two fluids. The compressibility of a two-phase fluid composed of gas and gas-saturated brine is between that of a gas and that of a brine and depends on the relative proportions of the two fluids. Osif (1988) presents extensive new data on the compressibility of mixed gas–brine systems.

Flow-limited propagation

Infiltration-limited and compressibility-limited models assume that the crack tip propagates slowly enough to maintain contact with fluid inside the joint. For these two models, the rate of fluid flow from the preexisting part of the joint into the newly created portion of the joint is faster than the speed of joint propagation. If the crack tip is

restrained and is suddenly released, the crack, at least momentarily, becomes unstable. In this case, the crack may outrun the fluid within the crack (Sammis and Julian, 1987). In the most extreme case of a flow-limited model the rate of fluid flow into the propagating joint tip is infinitely slow relative to the rate of joint propagation. A case similar to this is described by Secor and Pollard (1975). Cracking under conditions where flow to the tip is limited is roughly equivalent to inserting a flat-jack into a slot and pressurizing it until rupture occurs. Velocity of the crack tip increases because K_I increases with crack length. The crack may arrest for one or both of two reasons: (1) The dry crack tip may outrun the zone in which the stresses generated by the pressurized portion of the crack overcome the remote crack normal compressive stresses. (2) Enough fluid may drain into the crack tip so that the driving stress is relieved. This mechanism necessarily leads to cycling, although the time between cycles could be short if fracturing resumes immediately upon equilibration of fluid pressure. This model for incremental crack growth is rejected as indicated by discussion in the next section.

4. Discussion: Mechanism of Cyclic Crack Propagation in the Ithaca Siltstone

4.1. Causes of instability and crack front acceleration

This section considers possible mechanisms to explain crack front acceleration during formation of an increment. Infiltration-limited propagation is not compatible with cyclic crack propagation in the Ithaca Siltstone because crack velocity increased during each cycle and because of the low permeability of the siltstone (Table 1). The boundary between increments 0 and 1 or possibly between increments 1 and 2 marks the onset of cyclic propagation of the study joint after an initial period of steady-state infiltration-limited propagation. Concerning the flow-limited model, Sammis and Julian (1987) show that, if an isolated flat crack with a dry tip is subjected to a far-field compression, it will not propagate unstably when its internal fluid pressure increases. Finally, the relationship between K_I and fluid pressure for the case of a crack with uniform fluid pressure is given by eq. (4). Inspection of eq. (4) shows that an increase of crack fluid pressure is necessary to increase K_I. Acceleration of the fracture is, therefore, prohibited for all of the models because there is a decline of fluid pressure during propagation. However, morphological evidence suggests that the fracture velocity increased during each cycle. If so, then before propagation began, the fluid pressure must have risen above the critical fluid pressure required to propagate the crack. Hence, the crack tip must have been restrained in some way so that the buildup of fluid pressure could occur without being dissipated by subcritical extension of the study joint. We can imagine several possible sources for this restraint.

The tendency for the study joint front to be convex in the propagation direction shows that bedding-plane tractions influenced propagation. It is possible that bedding tractions may have helped restrain the tip after propagation ceased. However, bedding tractions should have been less effective at restraining the stationary fracture tip than the moving tip because creep along the bedding planes while the fracture front was stationary should have allowed relaxation of the bedding tractions. Since bedding plane

tractions did not prohibit dynamic propagation, this is an unlikely mechanism for stationary crack-tip restraint.

Other possible restraining mechanisms have their origin in the geometry of the crack tip. Small-scale irregularities of the arrest lines could have served to restrain the tip somewhat. Arrest lines have a coarser texture than the remainder of the crack and some are slightly curved. The roughness resulting from the presence of numerous fracture tongues may have effectively produced a larger radius of curvature of the crack tip. This effect could have inhibited reinitiation by decreasing the stress concentration and thereby increasing the pressure required to reinitiate cracking. A short, bent tip would also restrain crack propagation. But rough calculations using stress intensity factors for cracks with an infinitesimally short bent tip (Murakami, 1987) and $\sigma(\theta)_{max}$ theory (Erdogan and Sih, 1963; Ingraffea, 1987) show that for a tip deviation of 1–3° out of the crack plane the propagation pressure is increased by 0.01 to 0.6 Pa for joints with c between 10 and 100 m. Thus, bent tips provide only a small contribution to the overpressure, although the calculation did not take into account the crack parallel compressive loads. If a joint turns out of parallel with the principal compressive stress, the pressure required to propagate the crack increases because of the resolved compression across the tip.

A scenario for incremental propagation can be envisioned if subcritical propagation returned the crack to its optimal orientation while the fluid pressure built. Once the optimal orientation was achieved, the crack tip was released and the crack could accelerate because K_I was slightly above K_{IC}. As above, crack arrest occurred when the fluid pressure drop inside the crack caused the stress intensity to decline to K_{IC}. Formation of the arrest line then began the process anew. It is possible that the development of the complex boundary between increments 0 and 1 (Figure 3) could have initiated this process, which then became self-perpetuating. However, such a tip-restraint model seems unlikely because of the small amount of overpressure that the arrest lines can provide and because the complex fracture progression seen in Figure 3 does not seem to favor such a delicate balance.

Another explanation for the velocity increase is that the fracture toughness of the rock declined during a propagation cycle. Some materials show decreased fracture toughness with increasing fracture velocity (Broek, 1987). Such rate-dependent effects may have amplified the effects of crack tip restraint to produce the velocity increase. These dynamic fracture toughness changes could have led to acceleration under a steadily declining load. This hypothesis is impossible to test for the Ithaca Siltstone owing to a lack of relevant data.

In the next subsection we argue that a pressure drop of 1–5 MPa occurred during a propagation event. None of the above mechanisms explain this much overpressure. Another possibility is that interactions between the study joint and adjacent fractures provided a trigger for cyclic propagation. Propagation of a nearby joint could have resulted in a pressure drop within that joint and thereby decreased the total horizontal stress on the walls of the study joint. A drop in total horizontal stress may have released the study joint tip and thus initiated a propagation increment. Cyclic propagation may have begun when adjacent joints began to interfere. The large size of increment 1 may result from the transition from steady-state infiltration-limited propagation to cyclic propagation. Weak crack-tip interactions with an adjacent joint may have produced the complex geometry of the arrest lines between increments 0 and 1 and between increments 1 and 2.

4.2. Pressure-drop during increment formation

The pressure in excess of σ_h (the minimum horizontal total stress) that is required to drive a joint is the result of fracture toughness (eqs. 4 and 5). Longer fractures require a lower excess pressure if the fracture is modeled as an isolated penny-shaped crack or infinite flat tunnel crack in a homogeneous medium. These models assume that all parts of the fracture 'feel' all other parts of the fracture through the elastic medium. This may not be an appropriate model for the study joint. The study joint was confined to a single bed that was quite thin relative to the length of the study joint. Tractions along the bounding bedding planes may have resulted in mechanical isolation of the crack tip so that joint behavior was independent of joint size. If this was the case, only a portion of the fracture (the 'effective length') was mechanically coupled to the crack tip. Size-independent behavior of large fractures has been observed in some cases of failure of large engineering structures such as boilers and pipelines (Broek, 1987). Also, size-independent fracture behavior is assumed in the widely used PKN model for artificial hydraulic fractures that are confined to a single bed (Perkins and Kern, 1961; Nordgren, 1972; see Ben-Naceur, 1989 for a recent review of artificial hydrofrac models). We postulate that the study joint exhibited such size-independent behavior.

Size-independent behavior implies that the internal joint pressure required to drive the fracture must have been essentially constant once the joint reached a certain size. A maximum value for the pressure in excess of σ_h required to drive a joint within the bed that contained the study joint may be obtained by assuming that the effective length was equal to the bed thickness and that a penny-shaped geometry is appropriate for the crack tip (eq. 4). This calculation gives an excess pressure of 5.2 MPa. The propagation-induced pressure drop of a joint within this bed could not have exceeded the excess pressure in any case, so that joint interactions could have provided no more than about 5 MPa of overpressure for incremental propagation of the study joint. During cyclic propagation of the study joint the value of K_I must have remained close to K_{IC} because the fracture velocity never rose sufficiently high for branches to form (see Appendix Figure 12; preceding discussion), so that the pressure drop within the study joint during incremental propagation must therefore have been small. We suggest that 'small' was on the order of 5 MPa.

4.3. Hydraulic drive mechanism

Sammis and Julian (1987) provide an equation applicable for evaluating the stress intensity for our flow-limited model at the tip of an isolated flat tunnel crack in compression with internal fluid pressure and dry tips. Solving this for the fluid pressure within the wet part of the crack after the formation of a dry increment gives

$$P = \frac{K_{IC} + \sigma_h[\pi(c + \Delta c)]^{1/2}}{2[(c + \Delta c)/\pi]^{1/2} \sin^{-1}[c/(c + \Delta c)]} \tag{1}$$

for a vertical joint, where c is the crack half-length, Δc is the length of the dry tips, P is the crack fluid pressure, and σ_h is the crack perpendicular compressive stress.

Equations (1) and (5) were solved for the fluid pressure in excess of σ_h for values of c between 1 and 1000 m and for $\Delta c = 0.6$ m, which is the normalized length of the initial large propagation increments on the study joint face. Comparison of the results shows that the propagation pressure for a joint with a dry tip is 35–19 times greater than the

propagation pressure of a uniformly pressurized fracture *after* the formation of the increment. At fracture initiation the fluid pressure must have been much higher. This calculation underestimates the required initial joint pressure for two reasons. The calculation was performed for the pressure after formation of the increment and the calculation was performed for an infinite tunnel crack that was larger than the likely effective length of the study joint. It is unlikely that any possible crack-restraint mechanisms could have provided enough restraint for the fluid pressure to build to levels sufficient for flow-limited fracturing to occur or that a significant length of dry crack could exist during propagation. We discard the flow-limited fracturing model as a possible drive mechanism and, hence, favor the compressibility-limited propagation model by elimination. The sections below show that the compressibility-limited propagation model leads to reasonable predictions of the cycling behavior and allows identication of the driving fluid within the study joint.

4.4. Identification of the joint-forming fluid

Specific predictions about the size increments associated with a given fracture length are obtained from the compressibility-limited model. One way to quantitatively evaluate our model is with the PKN model for artificial hydrofracs (Perkins and Kern, 1961; Nordgren, 1972). The PKN model is appropriate for a long, vertical fracture confined to a single bed with the fracture length in bedding much greater than the bed thickness (Figure 10). In the PKN model, the fracture pressure varies slowly along the length of the fracture, so that the aperture of any cross-section is controlled by the pressure within the fracture at that point. The geometry of a given section of the fracture is then computed by idealizing it as a two-dimensional pressurized elliptical hole (Nordgren, 1972). The area of an ellipse is given by

$$\text{Area} = \pi ab \tag{2}$$

where a is the semimajor axis of the ellipse (in this case half the bed height), and b is the semiminor axis of the ellipse (in this case half the fracture aperture at the bed center).

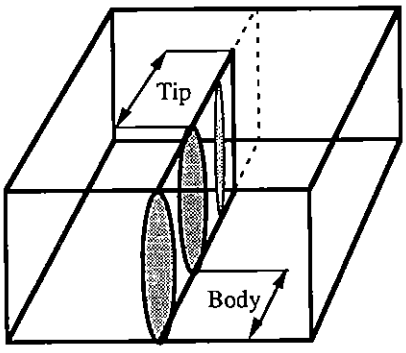

Figure 10. Geometry of the PKN fracture model as applied here. The body has a constant cross-sectional area because the fluid pressure throughout the fracture is uniform while the tip has a uniform taper due to toughness effects and tip restraint.

b is given by (Nordgren, 1972; Pollard and Segall, 1987)

$$b = \frac{2Pa(1 - \nu^2)}{E} \tag{3}$$

where P in this case is the amount by which the crack pressure exceeds σ_h. The driving stress, P, equals the driving stress, σ, as computed from eq. (4) in the Appendix. The cross-sectional area is thus constant for the case in which the pressure is uniform along the fracture, and the fracture volume is therefore equal to the fracture length times the cross-sectional area. Equations (2) and (3) were evaluated for this case using the data in Table 1.

The PKN model for artificial hydrofracs is developed in terms of the injection and flow rates of fluid within the crack from the wellbore so that the crack volume is dependent on the pressure distribution. In the compressibility-limited propagation model, the pressure is uniform throughout the fracture, so that the volume of the fracture tip region is controlled by bedding tractions and fracture toughness. To obtain an estimate of a newly formed tip segment, we assume that the segment has a uniform taper and a triangular cross-section parallel to bedding so that the volume of an increment at the crack tip is half the volume of an equivalent length of the main portion of the fracture body. Propagation leads to formation of a new increment of similar length and expansion of the old increment to a cross-section equivalent to that of the rest of the fracture. The total increase of the crack volume during propagation is therefore equal to the cross-sectional area of the main fracture body times the increment length. We assume that contraction of the main fracture body due to the propagation-induced pressure drop is negligible. This is a valid approximation because inward movement of the joint walls near the tip would result in arrest.

Any geologic fluid, either liquid, gas, or mixtures of the two, may drive a joint. In sedimentary rocks, brine and natural gas are typical pore fluids, which we will use to evaluate the compressibility-limited propagation model. We discuss natural gas in terms of pure methane and brine in terms of pure water in the arguments that follow. The depth of burial of the Ithaca Siltstone was about 3 km at the time of joint formation (Engelder and Lacazette, 1990) so that the temperature was about 90–105°C given a geotherm of 25–30°C km^{-1}. Under the pressure and temperature conditions assumed for joint propagation at Watkins Glen, the adiabatic compressibility of methane is about 1.5% MPa^{-1} (Figure 11; Angus et al., 1976), while the compressibility of water is about 0.04% MPa^{-1} throughout the pressure–temperature region of interest (Sato et al., 1988). If the driving fluid was methane and the final fracture length was 90 m, then the final 1 m long increments could have been driven by a pressure drop of 0.74 MPa, which is within the acceptable limits defined above. If the driving fluid was water, then a 27 MPa pressure drop during propagation is required to drive the final increments, which is 520% higher than the maximum estimate of 5.2 MPa that is derived above and is between 30% and 50% of the total horizontal stress, depending on the exact overburden thickness at the time of propagation.

The size of the study joint during propagation of the initial increments is not well-constrained because asymmetrical propagation is observed on joints in this outcrop. The study joint may have experienced unequal growth on either end. It is possible to estimate the minimum initial size of the study joint at the onset of cycling by noting that the study joint was at least 13 m long when cycling began (Figure 3). Choosing methane as the crack fluid leads to a pressure drop of 3.1 MPa during increment

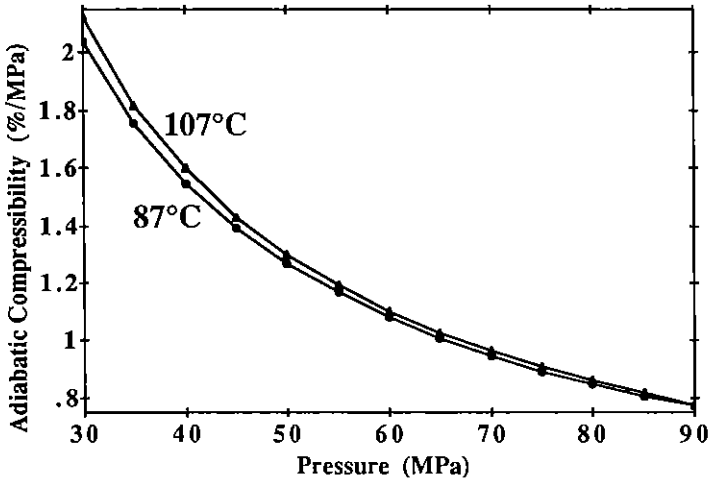

Figure 11. Adiabatic compressibility of methane as a function of pressure at two different temperatures, as calculated from the data of Angus et al. (1976).

formation, while water requires a 115 MPa pressure drop. Water is clearly too incompressible to have served as the crack fluid.

Although water is unacceptable as a driving fluid for the study joint, the data are not adequate to distinguish between geologically common gases or to resolve whether or not the fluid was actually a two-phase mixture with a small liquid fraction. It is unlikely that a liquid fraction was present, because the joints show no evidence of fill or mineralization of any kind. A natural gas with a substantial methane component is the most likely driving fluid for several reasons: (1) the Ithaca Siltstone beds that contain these joints are enclosed in organic-rich black shales and the beds themselves are black to dark gray, presumably from organic matter; (2) the temperature of the rocks at the time of joint formation was appropriate for methanogenesis; (3) natural gas is presently produced from adjacent formations in the region.

We explain the increase in size of the increments with increasing fracture length by postulating that joint growth led to a larger joint volume so that progressively larger increments were driven as the study joint grew. In the pressure–temperature region of interest the compressibility of methane changes over 100% as a function of pressure (Figure 11) whereas the compressibility of water changes by about 15% as a function of pressure (Sato et al., 1988). Formation of the joint set would have resulted in concomitant drainage of the pore fluid into the crack so that the pore pressure behind the study joint would have declined as the joint set grew. Drainage would then have led to a decrease in the total earth stress on the study joint wall and a decrease in the propagation pressure of the study joint (eq. 8). The tendency toward larger increments with increasing joint length is favored by both the change in compressibility of the driving fluid and the increase in joint size. A natural-gas drive provides a more effective mechanism than a water drive for increasing increment size as a function of joint length because of the larger compressibility change of methane in response to decreasing pressure. However, we cannot quantitatively assess this effect without better knowledge of fluid composition, stress state, fluid-pressure regime, and joint size during joint growth.

4.5. Work of joint formation

The three models discussed above are developed in terms of the hydraulic controls on the driving stress of the joint. The work of joint propagation may be understood by considering the joint and rock as a fixed-grips system. During a propagation event the remote boundaries of the rock mass do not move, but the driving stress relaxes. The driving stress for joint propagation is supplied by the fluid pressure within the joint because the crack normal stress in the earth is compressive. When a joint propagates, the work of fracture is supplied by the PV work done by the fluid within the joint and by the release of stored elastic strain energy in the rock mass. A hydraulic criterion is therefore sufficient to describe the stress of cracking but is insufficient to describe the energy balance. Both work and stress conditions must be met for a valid model of fracture behavior (Broek, 1987).

The amount of work available from expansion of methane increases with declining pressure under the conditions at which the study joint formed, and may provide another way to understand the increase in increment size. The isenthalpic Joule–Thomson coefficient (μ) is equal to $(dT/dP)_H$ for a fluid. For methane in the temperature and pressure range at which the joint propagated, μ changes sign with increasing pressure, so that at higher pressure the temperature increases on expansion while at lower pressure the temperature decreases on expansion. Less work can be extracted from methane at higher pressures because of this effect. Decreasing pressure during joint propagation would therefore have led to an increase in the amount of work that methane could do on the joint walls by expansion. If methane was the driving fluid, then increasing increment size is favored from the standpoint of the energy balance of fracturing. In contrast, μ is negative for water throughout the P–T region of interest (so that heating occurs on expansion) and increases only slightly with declining pressure (Grigull et al., 1968). Again, this aspect cannot be evaluated quantitatively without better knowledge of the conditions of joint formation and fluid composition.

5. Conclusions

The three conceptual hydraulic models provide a useful framework in which to consider the hydraulic controls of joint propagation: infiltration of host-rock pore fluid into the joint, flow of the fluid within the joint, and the compressibility of the driving fluid.

The study joint in the Ithaca Siltstone initiated by slow, steady-state infiltration-driven propagation. The change to incremental propagation probably resulted from crack interactions.

The compressibility of the driving fluid appears to be the major control on increment size. Joints in the Ithaca Siltstone at Watkins Glen were driven by natural gas.

Acknowledgments

We thank Mike Gross and Paul Scott for help with field work. Art Rose and Steve Mackwell provided helpful reviews of early versions of this manuscript. Two anonymous reviewers provided helpful comments. This work was supported by an unrestricted grant to Terry Engelder from Texaco and by Gas Research Institute contract 5088-260-1746.

References

Anderson, O.L. and Grew, P.C. (1977). Stress corrosion theory of crack propagation with applications to geophysics. *Rev. Geophys. Space Phys,* **15**, 77–104.

Angus, S., Armstrong, B., and de Reuck, K.M. (1976). *International thermodynamic tables of the fluid state – 5*: Methane. International Union of Pure and Applied Chemistry Chemical Data Series. Pergamon Press, New York.

Atkinson, B.K. (1984). Subcritical crack growth in geological materials. *J. Geophys. Res.* **89**, 4077–4114.

Atkinson, B.K. (1987). Introduction to fracture mechanics and its geophysical applications. In *Fracture Mechanics of Rock* (ed. B.K. Atkinson), pp. 1–26. Academic Press, London.

Atkinson, B.K. and Meredith, P.G. (1987a). The theory of subcritical crack growth with applications to minerals and rocks. In *Fracture Mechanics of Rock* (ed. B.K. Atkinson), pp. 111–166. Academic Press, London.

Atkinson, B.K. and Meredith, P.G. (1987b). Experimental fracture mechanics data for rocks and minerals. In *Fracture Mechanics of Rock* (ed. B.K. Atkinson), pp. 477–525. Academic Press, London.

Bahat, D. and Engelder, T. (1984). Surface morphology on cross-fold joints of the Appalachian Plateau, New York and Pennsylvania. *Tectonophysics* **104**, 299–313.

Beach, A. (1977). Vein arrays, hydraulic fractures, and pressure solution structures in a deformed flysch sequence, S.W. England. *Tectonophysics* **40**, 201–225.

Ben-Naceur, K. (1989). Modeling of hydraulic fractures. In *Reservoir Stimulation* (ed. M.J. Economides and K.G. Nolte), pp. 3-1–3-31. Prentice-Hall, Englewood Cliffs, N.J.

Broek, D. (1987). *Elementary Engineering Fracture Mechanics.* Martinus Nijhoff, Dordrecht.

Brown, S.R. and Scholz, C.H. (1985). Broad bandwidth study of the topography of natural rock surfaces. *J. Geophys. Res.* **90**, 12575–12582.

Costin, L.S. (1987). Time-dependent deformation and failure. In *Fracture Mechanics of Rock* (ed. B.K. Atkinson), pp. 167–216. Academic Press, London.

Engelder, T. (1985). Loading paths to joint propagation during a tectonic cycle: An example from the Appalachian Plateau, U.S.A. *J. Struct. Geol.* **7**, 459–476.

Engelder, T. (1986). The use of joint patterns for understanding the Alleghanian orogeny in the Upper Devonian Appalachian Basin, Finger Lakes district, New York. In *New York State Geological Association 58th Annual Meeting Field Trip Guidebook*, pp. 129–144.

Engelder, T. (1987). Joints and shear fractures in rock. In *Fracture Mechanics of Rock* (ed. B.K. Atkinson), pp. 27–70. Academic Press, London.

Engelder, T. and Lacazette, A. (1990). Natural hydraulic fracturing. In *Rock Joints* (ed. N. Barton and O. Stephansson), pp. 35–43. A.A. Balkema, Brookfield.

Erdogan, F. and Sih, G.C. (1963). On the crack extension in plates under plane loading and transverse shear. *ASME J. Basic Eng.* **85** (Dec.), 519–527.

Evans, K., Oertel, G., and Engelder, T. (1989). Appalachian stress study 2: Analysis of Devonian shale core: some implications for the nature of contemporary stress variations and Alleghanian deformation in Devonian rocks. *J. Geophys. Res.* **94**, 7155–7170.

Freiman, S.W. (1984). Effects of chemical environment on slow crack growth in glasses and ceramics. *J. Geophys. Res.* **89**, 4072–4076.

Fyfe, W.S., Price, N.J., and Thompson, A.B. (1978). *Fluids in the Earth's Crust.* Elsevier Scientific, New York.

Geiser, P.E. and Sansone, S. (1981). Joints, microfractures, and the formation of solution cleavage in limestone. *Geology* **9**, 280–285.

Gretener, P.E. (1981). Pore pressure: Fundamentals, general ramifications, and implications for structural geology. *American Association of Petroleum Geologists Educational Course Note Series 4.*

Grigull, U., Bach, J., and Reimann, M. (1968). Die eigenshaften von Wasser und Wasserdampf

nach 'The 1968 IFC Formulation.' *Wärme und Soffübertragung* **1**, 202–213.
Helgeson, D. and Aydin, A. (1988). Composite joints in layered sedimentary rocks: implications for fracture permeability. Geological Society of America Abstracts with Programs 20, A318.
Helgeson, D. and Aydin, A. (1989). Use of surface features for interpretation of the propagation, interaction, and intersection of joints. Geological Society of America Abstracts with Programs 21, A64.
Ingraffea, A.R. (1987). Theory of crack initiation and propagation in rock. In *Fracture Mechanics of Rock* (ed. B.K. Atkinson), pp. 71–110. Academic Press, London.
Jaeger, J.C. and Cook, N.G.W. (1979). *Fundamentals of Rock Mechanics*, 3d edn. Chapman and Hall, New York.
Kulander, B.R., Barton, C.C., and Dean, S.L. (1979). *The Application of Fractography to Core and Outcrop Fracture Investigations.* U.S. Dept. of Energy, Morgantown, National Technical Information Service # METC/SP-79/3.
Kulander, B.R. and Dean, S.L. (1985). Hackle plume geometry and joint propagation dynamics. In *Fundamentals of Rock Joints.* (ed. O. Stephansson), pp. 85–94. Centek Publishers, Sweden.
Lawn, B. (1983). Physics of fracture. *J. Am. Ceramic Soc.* **66**, 83–91.
Lawn, B.R. and Wilshaw, T.R. (1975). *Fracture of Brittle Solids.* Cambridge University Press.
Michalske, T.A. (1983). The stress corrosion limit: Its measurements and implications. In *Fracture Mechanics of Ceramics*, vol. 5 (ed. R.C. Bradt, A.G. Evans, D.P.H. Hasselman, and F.F. Lange), pp. 277–289. Plenum Press, New York.
Murakami, Y. (ed.) (1987). *Stress Intensity Factors Handbook* (two volumes). Pregamon Press, Oxford.
Nordgren, R.P. (1972). Propagation of vertical hydraulic fractures. *Soc. Petrol. Eng.* **12**(4), 306–314.
Nur, A. and Byerlee, J.D. (1971). An exact effective stress law for elastic deformation of rocks with fluids. *J. Geophys. Res.* **76**, 6414–6419.
Osif, T.L. (1988). The effects of salt, gas, temperature and pressure on the compressibility of water. *Soc. Petrol. Eng. Reservoir Eng.* **3**, 175–181.
Olson, J. and Pollard, D.D. (1989). Inferring paleostresses from natural fracture patterns: A new method. *Geology* **17**, 345–348.
Perkins, T.K. and Kern, L.R. (1961). Widths of hydraulic fractures. *J. Petroleum Technol.* **13**, 937–949.
Pollard, D.D. and Segall, P. (1987). Theoretical displacements and stresses near fractures in rock with application to faults, joints, veins, dikes, and solution surfaces. In *Fracture Mechanics of Rock* (ed. B.K. Atkinson), pp. 277–349. Academic Press, London.
Ramsay, J.G. (1980). The crack-seal mechanism of rock deformation. *Nature* **284**, 135–139.
Sammis, C.G. and Julian, B.R. (1987). Fracture instabilities accompanying dike intrusion. *J. Geophys. Res.* **92**, 2597–2605.
Sato, H., Uematsu, M., Watanabe, K., Saul, A., and Wagner, W. (1988). New international skeleton tables for the thermodynamic properties of ordinary water substance. *J. Phys. Chem. Ref. Data* **17**, 1439–1540.
Scott, P.A. (1989). Analysis of the correlation between fracture toughness and surface roughness on joints in the Ithaca Siltstone, Watkins Glen, New York. M.S. thesis, The Pennsylvania State University.
Secor, D.T. (1965). Role of fluid pressure in jointing. *Am. J. Sci.* **253**, 633–646.
Secor, D.T. (1969). Mechanics of natural extension fracturing at depth in the earth's crust. *Geological Survey of Canada Paper 68-52*, pp. 3–48.
Secor, D.T. and Pollard, D.D. (1975). On the stability of open hydraulic fractures in the earth's crust. *Geophys. Res. Lett.* **2**, 510–513.
Segall, P. and Pollard, D.D. (1983). Joint formation in granitic rock of the Sierra Nevada: *Geological Society of America Bulletin 94*, pp. 563–575.
Tada, H., Paris, P., and Irwin, G. (1973). *The Stress Analysis of Cracks Handbook.* The Del Research Corporation, Hellertown, Pennsylvania.

Appendix: Fundamental Concepts of Fracture Mechanics and Joint Propagation

A.1. Joint initiation and propagation

Many textbooks and review articles provide an introduction to fracture mechanics (Lawn and Wilshaw, 1975; Broek, 1987; Atkinson, 1987). Chemical environment influences the velocity of crack propagation (Anderson and Grew, 1976; Atkinson, 1984; Atkinson and Meredith, 1987a). Stresses and displacements around ellipsoidal fractures are considered in detail by Pollard and Segall (1987). Fracture mechanics data for rocks and minerals are reviewed and summarized by Atkinson and Meredith (1987b). The discussion below considers only the case of pure mode I (tensile) fracture, which is commonly referred to as 'cracking.' In this paper the term 'joint' is used to describe a natural mode I rock fracture (i.e., a crack). The discussion here is framed in terms of linear elastic fracture mechanics, which assumes a linearly elastic–perfectly brittle material. Although these are excellent approximations for cracks in single crystals and for microscopic cracks in polycrystalline materials (Lawn, 1983; Atkinson, 1987), nonlinear effects are possibly significant in cases of natural rock fracture where the crack is large relative to the grain size (Ingraffea, 1987; Scott 1989; Scott et al., this volume, Chapter 16). Nevertheless, linear elastic fracture mechanics provides useful first-order approximations of the fracture behavior of rock.

In the general case of tensile fracture, the crack tip stress intensity is described by

$$K_I = -Y\sigma c^{1/2} \tag{4}$$

where K_I (i.e., K-one) is the stress intensity factor at the crack tip, Y is a geometric factor that accounts for the crack shape and loading condition, c is the crack half-length, and σ is the driving stress (compression considered positive). In this paper the driving stress is the superposition of the crack fluid pressure and the crack perpendicular earth stress. For a penny-shaped (circular disk) crack, $Y = 1.13$, while for an infinite flat tunnel crack, $Y = 1.77$ (Broek, 1987). K_I will increase with an increase in either crack length or driving stress. In order for K_I to remain constant during crack propagation the driving stress must fall. Equation (4) contains no information about the material in which the crack is contained. The critical stress intensity or mode I fracture toughness (K_{IC}) is a material property that expresses the stress intensity at which a crack propagates unstably in a given material.

If the driving stress is supplied by fluid pressure within the fracture, this fluid pressure must counterbalance both the rock strength (eq. 4) and the compressive stress acting on the joint wall. The classic model for fluid-driven joint initiation and propagation was developed by Secor (1965, 1969) who postulates that fractures initiate from randomly oriented Griffith flaws which are loaded by the in-situ pore fluid. Secor (1965, 1969) assumes that the only stress that the fracture pressure must overcome is σ_3, the least principal far-field compressive stress. Price (in Fyfe et al., 1978) and more recently Gretener (1981) have correctly pointed out that, for the propagation of vertical cracks, this analysis neglects the role of pore pressure in increasing the total stress. Fyfe et al. (1978) recognize that Secor's (1965, 1969) mechanism is viable for vertical cracks if the general law of effective stress (Nur and Byerlee, 1971) is used in place of the simple law. Engelder and Lacazette (1990) clarify this concept and develop equations to describe

joint initiation and propagation based on linear elastic fracture mechanics and the equations of poroelasticity. The key difference is that across vertical cracks there is a poroelastic term that must be added to the fracture pressure equation so that

$$P_f = \frac{K_{IC}}{Yc^{1/2}} + \sigma_3 + \alpha P_p \tag{5}$$

where P_f is the fluid pressure within the crack or flaw that is required to cause propagation, α is Biot's poroelastic constant, and P_p is the in-situ pore pressure of the rock mass. It is important to note that in this paper the sign conventions differ from those of Engelder and Lacazette (1990). In eqs. (4–8) both pressure and compressive stress have positive signs. Although this convention differs from that which is normally employed in the engineering literature, it is more convenient for the calculation of the fluid pressure required to propagate the crack.

Secor's (1965, 1969) original model and Engelder and Lacazette's (1990) modification postulate that at joint initiation, P_f is equal to P_p. It is implicit in the model that P_p exceeds σ_3 so that a condition of effective tension exists at fracture initiation. P_p must also exceed the least principal total stress. The average stress within the solid skeleton of the rock (the total stress) has two components: remotely applied load (σ_3) and porelastically derived stress that results from P_p (which is given by αP_p). During cracking, part of P_p must counterbalance the applied loads while the remainder must counterbalance its own contribution to the average skeletal stress. This contribution arises because the solid skeleton of the rock is not free to expand in response to P_p. A flaw can propagate under these circumstances because it is much larger than an individual grain or pore and because αP_p is >0 and $<P_p$ for consolidated materials such as rocks. The wall of the flaw thus feels the full effects of P_p acting outward, while only part of P_p acts inward through the solid skeleton of the rock. Cracking occurs when P_p exceeds the sum of the far-field stress and its own contribution to the average skeletal stress. The amount by which P_p must exceed the sum of the inward-acting stresses is a function of the size and geometry of the flaw and the fracture toughness of the rock. This process of natural hydraulic fracturing may not be viable at the scale of individual grains and pores, where a complex stress state may exist. In the Ithaca Siltstone the origin flaws of joints are roughly 1–3 cm in size (Engelder and Lacazette, 1990).

Engelder and Lacazette (1990) define a tectonically relaxed basin as one where σ_2 and σ_3 are equal, horizontal, and a function of the overburden load so that

$$\sigma_2 = \sigma_3 = \frac{\nu}{1-\nu}\sigma_{ve} \tag{6}$$

where σ_{ve} is the effective vertical stress supplied by the overburden load and ν is Poisson's ratio. σ_{ve} is given by

$$\sigma_{ve} = \sigma_v - \alpha P_p \tag{7}$$

σ_v is equal to the weight of the saturated overburden. In a tectonically relaxed basin, eq. (5) becomes

$$P_f = \frac{K_{IC}}{Yc^{1/2}} + \frac{\nu}{(1-\nu)}\sigma_v + \frac{1-2\nu}{1-\nu}\alpha P_p \tag{8}$$

A.2. Crack velocity

Crack velocity in a linear elastic rock is a function of K_I (Anderson and Grew, 1977). Slow, stable crack propagation occurs at lower values of K_I. When $K_I = K_{IC}$, the critical stress intensity, the fracture is unstable and the velocity undergoes large increases with small increases of K_I. This behavior is shown schematically in Figure 12. The term subcritical crack propagation describes fracturing when $K_I < K_{IC}$. Subcritical crack growth mechanisms in rocks and minerals are reviewed by Costin (1987) and Atkinson and Meredith (1987a). These mechanisms include stress corrosion, dissolution, diffusion, ion-exchange, and microplasticity, although stress corrosion is the dominant mechanism by which subcritical cracking occurs in geologic materials. All of these mechanisms are affected by the chemical environment of the crack; however, microplasticity and defect diffusion may also occur in a vacuum.

In a chemically mediated process, such as stress corrosion, the controlling process is the rate of chemical reactions at the crack tip. In the subcritical regime, dramatic changes in crack velocity accompany changes in the mechanism of cracking (Figure 12) thus producing the three regions of the velocity curve in Figure 12 (Atkinson, 1984). At very slow crack velocities the crack behavior is controlled by the rate of reactions at the crack tip (Region I). As the crack-tip velocity increases it reaches the diffusion rate of reactive species to the crack tip (Region II). Velocity in Region II is unaffected by changes in K_I if diffusion-controlled rupture operates. In Region III, K_I approaches K_{IC} and the crack velocity increases to the point where the crack tip outruns the effects

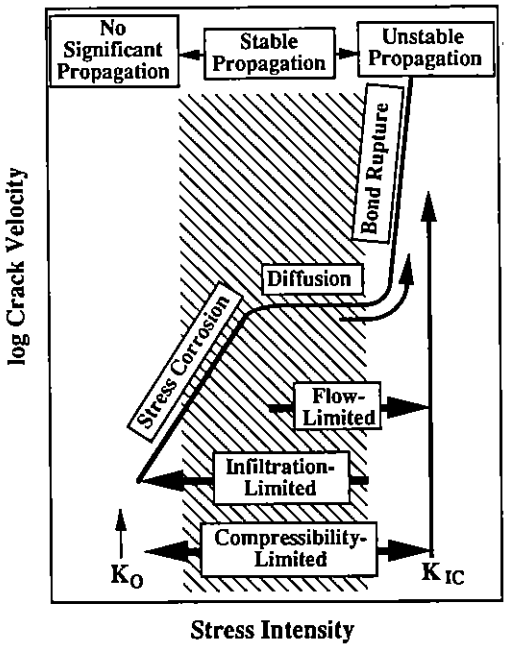

Figure 12. Schematic stress intensity vs. crack velocity diagram (after Atkinson, 1984). Diagram also shows the velocity fields appropriate to the three hydraulic models presented in Figure 9.

of the chemical environment so that crack tip behavior is controlled by bond rupture alone. K_{IC} is therefore essentially independent of chemical environment (Freiman, 1984). Although it has not been demonstrated in geologic materials that there is a limiting value of K_I below which no crack growth occurs (Atkinson, 1987), the existence of such a limit has been proven for glasses (Michalske, 1983). The subcritical crack growth limit is termed K_0 (Figure 12).

Three states in the subcritical regime pertain to the rate of joint propagation: no significant crack propagation; stable crack propagation; and unstable crack propagation (Figure 12). Although crack propagation does occur in the field of no significant propagation, it contributes very little to the overall growth of a crack increment. Stable crack propagation occurs if the change in crack length and the crack driving stress are balanced in such a manner that K_I does not increase abruptly. If K_I somehow increases abruptly then an unstable situation can develop where at least momentarily the crack-tip velocity increases greatly. Such a situation develops if the driving stress is maintained during crack propagation. For the development of cross-fold joints in the Ithaca Siltstone, K_I may have varied between the stress corrosion crack growth limit (K_0) and some value approaching K_{IC} (2.66 MPa $m^{1/2}$) as measured by Scott et al. (this volume, Chapter 14; Scott, 1989). Stable crack propagation is possible for a large range of K_I.